

RESEARCH ARTICLE

Instability of brain connectivity during nonrapid eye movement sleep reflects altered properties of information integration

Yi-Chia Kung¹  | Chia-Wei Li² | Shuo Chen³ | Sharon Chia-Ju Chen⁴ |
 Chun-Yi Z. Lo⁵ | Timothy J. Lane^{6,9,11}  | Bharat Biswal^{7,8}  |
 Changwei W. Wu^{6,9,11}  | Ching-Po Lin^{1,10}

¹Department of Biomedical Imaging and Radiological Sciences, National Yang-Ming University, Taipei, Taiwan

²Department of Radiology, Wan Fang Hospital, Taipei Medical University, Taipei, Taiwan

³Department of Biomedical Sciences and Engineering, National Central University, Taoyuan, Taiwan

⁴Department of Medical Imaging and Radiological Sciences, Kaohsiung Medical University, Kaohsiung, Taiwan

⁵Institute of Science and Technology for Brain-Inspired Intelligence, Fudan University, Shanghai, China

⁶Graduate Institute of Mind, Brain and Consciousness, Taipei Medical University, Taipei, Taiwan

⁷Department of Biomedical Engineering, New Jersey Institute of Technology, Newark, New Jersey

⁸Clinical Hospital of Chengdu Brain Science Institute, MOE Key Laboratory for Neuroinformation, University of Electronic Science and Technology of China, Chengdu, China

⁹Brain and Consciousness Research Center, Shuang-Ho Hospital, New Taipei, Taiwan

¹⁰Institute of Neuroscience, National Yang-Ming University, Taipei, Taiwan

¹¹Graduate Institute of Humanities in Medicine, Taipei Medical University, Taipei, Taiwan

Correspondence

Changwei W. Wu, 12 Floor, 172-1, Sec. 2, Keelung Street, Da-An District, Taipei 106, Taiwan.
 Email: sleepbrain@tmu.edu.tw

Ching-Po Lin, Institute of Neuroscience, National Yang-Ming University, Taipei, Taiwan.
 Email: chingpolin@gmail.com

Funding information

Ministry of Science and Technology, Taiwan.

Abstract

Nonrapid eye movement (NREM) sleep is associated with fading consciousness in humans. Recent neuroimaging studies have demonstrated the spatiotemporal alterations of the brain functional connectivity (FC) in NREM sleep, suggesting the changes of information integration in the sleeping brain. However, the common stationarity assumption in FC does not satisfactorily explain the dynamic process of information integration during sleep. The dynamic FC (dFC) across brain networks is speculated to better reflect the time-varying information propagation during sleep. Accordingly, we conducted simultaneous EEG-fMRI recordings involving 12 healthy men during sleep and observed dFC across sleep stages using the sliding-window approach. We divided dFC into two aspects: mean dFC (dFC_{mean}) and variance dFC (dFC_{var}). A high dFC_{mean} indicates stable brain network integrity, whereas a high dFC_{var} indicates instability of information transfer within and between functional networks. For the network-based dFC, the dFC_{var} were negatively correlated with the dFC_{mean} across the waking and three NREM sleep stages. As sleep deepened, the dFC_{mean} decreased ($N0 \sim N1 > N2 > N3$), whereas the dFC_{var} peaked during the N2 stage ($N0 \sim N1 < N3 < N2$). The highest dFC_{var} during the N2 stage indicated the unstable synchronizations across the entire brain. In the N3 stage, the overall disrupted network integration was observed through the lowest dFC_{mean} and elevated dFC_{var} , compared with N0 and N1. Conclusively, when the network specificity (dFC_{mean}) breaks down, the consciousness dissipates with increasing variability of information exchange (dFC_{var}).

KEYWORDS

consciousness, dynamic functional connectivity, functional magnetic resonance imaging (fMRI), integrated information theory (IIT), sleep

Grant/Award Numbers: MOST 104-2218-E-010-007-MY3, MOST 104-2420-H-038-001-MY3, MOST 105-2628-B-038-013-MY3, MOST 105-2632-H-038-001-MY3, MOST 106-2410-H-038-003-MY3, MOST 108-2420-H-010-001, MOST 108-2634-F-010-001; National Health Research Institutes, Grant/Award Number: NHRI-EX108-10611E; Science and Technology Commission of Shanghai Municipality, Grant/Award Numbers: 17JC1404101, 17JC1404105; National Natural Science Foundation of China (Young Scientists Fund), Grant/Award Number: 81801774; Natural Science Foundation of Shanghai, Grant/Award Number: 18ZR1403700

1 | INTRODUCTION

Sleep is associated with the fading of consciousness, with different states of consciousness being experienced every night during the various stages of sleep. Currently, sleep is classified into rapid eye movement (REM) and nonrapid eye movement (NREM) sleep (Iber, Ancoli-Israel, Chesson, & Quan, 2007). In contrast to the maintenance of consciousness during REM sleep, the level and content of consciousness in human is lost during NREM sleep (Hohwy, 2009; Laureys, 2005). NREM sleep can be further categorized into light sleep (i.e., the N1 and N2 sleep stages) and slow-wave sleep (SWS, also known as the N3 sleep stage) (Berry et al., 2012; Iber et al., 2007). With deepened NREM sleep stages, consciousness gradually decreases (Nir et al., 2013). In analyses of changing consciousness in NREM sleep, the breakdown and restoration of information integration are associated with the loss and recovery of consciousness (Tononi, 2004). The integrated information theory (IIT) originated from phenomenology, and has been used to identify consciousness and its association with physical systems (Tononi, 2004; Tononi, Boly, Massimini, & Koch, 2016). For example, when consciousness fades, the cortical responses become local (i.e., there is a loss of integration) or global but stereotypical (i.e., there is a loss of information) (Tononi & Koch, 2015). According to the IIT, brain network integrity is critical for information distribution and corresponding consciousness alterations.

In line with the fading consciousness that occurs during NREM sleep, neuroimaging studies have used brain functional connectivity (FC), that is, the functional MRI (fMRI) temporal coactivation between brain regions (Friston, 2011), to disclose the alterations in network integrity across NREM sleep stages (Nofzinger, Maquet, & Thorpy, 2013). For example, the brain networks take on a more randomized level of organization with decreased clustering values in the NREM sleep stage (Spoormaker et al., 2010). During SWS, the brain network organizations present as segregated network modules (Boly et al., 2012; Tagliazucchi et al., 2013a), implying a reduced ability for functional integration (Larson-Prior et al., 2011). However, previous FC studies in sleep neuroimaging were insufficient to support the IIT on the basis of the stationarity assumption without dynamic considerations. Moreover, during sleep, our brain connections consistently change in a spatiotemporal dimension, with such change being known as dynamic FC (dFC)

(Tagliazucchi & van Someren, 2017). Although numerous dynamic methods are available to reveal spatiotemporal brain activities, dFC using the sliding-window approach (Allen et al., 2012) can be related to EEG alterations (Chang, Liu, Chen, Liu, & Duyn, 2013) and associated with arousal (Chang et al., 2016), vigilance state (Thompson et al., 2013; Wang, Ong, Patanaik, Zhou, & Chee, 2016), and NREM sleep (Haimovici, Tagliazucchi, Balenzuela, & Laufs, 2017). In principle, the dFC across brain regions can better reflect the time-varying signal propagation, or information transfer, during sleep, given that the traveling spindle oscillations and slow waves between subcortex and neocortex (i.e., cross-region connectivity) have been found to be effective in the memory processing in NREM sleep (Czisch & Wehrle, 2009; Mulert & Lemieux, 2009; Steriade, 2003). Stemming from the active system consolidation, the reactivated memory traces elicited through hippocampal-cortical dialogs occur in a phase-locked manner, implying a raised instability of cross-region connectivity in NREM sleep (Buzsáki, 1996; Feld & Born, 2017; Rasch & Born, 2013). Recent studies have provided evidence that the dynamicity of brain integration across NREM sleep stages is potentially linked with the spontaneous processes of memory consolidation, emotion regulation, and consciousness variation (Amico et al., 2014; Tagliazucchi, Carhart-Harris, Leech, Nutt, & Chialvo, 2014). However, such dynamic alterations of brain connectivity are uncommon in wakefulness, and how dynamic information processing occurs across NREM sleep stages remains unclear. Based on the literature regarding NREM sleep, our working hypothesis is that the brain organizations experience multiple altered scenarios of information processing across wake-sleep stages and that these different scenarios can be reflected by the dFC index. To reveal the dFC across wake-sleep stages, we took a multivariate approach; that is, we took the mean of dFC (dFC_{mean}) as the measure of network integrity and the variance of dFC (dFC_{var}) as the measure of instability in network connectivity. Accordingly, we expected that dFC_{mean} would be decreased with the disruption of within-network connectivity in NREM sleep, while dFC_{var} would be increased with the increased instability of between-network information processing as NREM sleep deepens. Furthermore, both dFC_{mean} and dFC_{var} can be divided into within- and between-network components that better reflect the information integration from network perspectives (Beharelle, Kovačević, McIntosh, & Levine, 2012; Tononi, 2004).

2 | MATERIALS AND METHODS

2.1 | Participants

We recruited a total of 44 healthy young men to sleep naturally in an MRI scanner at National Yang-Ming University and collected data from 12 participants (age = 22.9 ± 2.5 years) with NREM sleep stages (see sleep architecture in Table S1). All of the participants were instructed to sleep for a regular duration of 7–8 hr per night, with consistent sleep and wake times, for at least 4 days, and the consumption of alcohol or caffeine-containing foods or drinks was prohibited on the day of the experiment. The exclusion criteria for the selection of participants were a habit of taking daytime naps, excessive daytime sleepiness, and a history of neurological or psychiatric disorders. Before scanning the participants, we collected their Pittsburgh Sleep Quality Index (PSQI) scores, including sleep quality, duration, and efficiency, to assess their sleep quality in the previous month. Before the experiment, each participant gave informed consent in accordance with the protocol approved by the National Yang-Ming University Institutional Review Board.

2.2 | Simultaneous EEG/fMRI recording

Simultaneous electroencephalography-functional magnetic resonance imaging (EEG–fMRI) signals were recorded for each functional scan. The EEGs were recorded using an MR-compatible system (Brain Products GmbH, Gilching, Germany) with 32-channels, which included 30 EEG channels, one electrooculography (EOG) channel, and one electrocardiogram (ECG) channel, all of which were positioned according to the international 10/20 system. The built-in impedance in each electrode was 5 k Ω and abrasive electrode paste (ABRALYT HiCI) was used to reduce the electrode-skin impedance to under 5 k Ω . The EEG signal was recorded synchronously with the MR trigger using Brain Vision Recorder software (Brain Products) with a 5-kHz sampling rate and a 0.5 μ V voltage resolution. A low-pass and a high-pass filter were set at 250 Hz and 0.0159 Hz, respectively, with an additional 60-Hz notch filter.

MRI data were collected using a 3T Siemens Tim Trio system (Erlangen, Germany) using a 12-channel head coil. High-resolution T_1 -weighted anatomical images (3D-MPRAGE with $192 \times 192 \times 176$ matrix size, 1 mm³ isotropic cube, flip angle (FA) = 9° repeat time (TR) = 1900 ms, echo time (TE) = 2.28 ms, and inverse time (TI) = 900 ms) were acquired before the functional scans for localization reference. Customized cushions were used to minimize head motion during each scan. Functional scans were subsequently acquired using a single-shot, gradient-recalled echo planar imaging (EPI) sequence (TR/TE/FA = 2,500 ms/30 ms/80°, field of view = 220 mm, matrix size = 64×64 , 35 slices with 3.4 mm thickness) aligned along the AC–PC line, thus allowing whole-brain coverage.

The experiment was conducted between 11 p.m. and 4 a.m. Before undergoing the MRI scans, the participants were tied with a pneumatic belt and an oximeter to simultaneously record Physiological Measurement Unit (PMU) data, which including respiration and cardiac pulsations. A T_1 -weighted anatomical image and resting-state

fMRI data were obtained before the sleep session. Participants were asked to attempt to fall asleep after the scan started. Termination criteria for the sleep session were (a) a scan time that reached the 125-min limitation for maintaining hardware stability and (b) a participant being unable to fall asleep for an extended period and choosing to terminate the session.

2.3 | Data preprocessing

Analyzer 2.0 (Brain Products, Germany) was used to preprocess the recorded EEG data offline. The preprocessing included down-sampling the EEG signal to 250 Hz and removing the gradient-induced artifact (adaptive average subtraction) and the ballistocardiographic artifact using the algorithm based on the R–R interval that was estimated by the ECG electrode. The electrodes were re-referenced to the averaged signal of all the EEG electrodes (Lei & Liao, 2017). The sleep stages were determined by the data from only four electrodes (C3, C4, O1, and O2). The resting-stage data acquired before each sleep session was regarded as wakefulness (N0). A licensed sleep technician from Kaohsiung Medical University Hospital visually scored the sleep stages (N1, N2, and N3) from the EEG data for every 30-s epoch, according to the criteria of the American Academy of Sleep Medicine (AASM) (Iber et al., 2007). Based on the sleep scoring, we extracted consecutive fMRI data for each of the four wake–sleep stages (including N0) in each participant. Each sleep stage contained continuous fMRI data lasting at least 4 min (96 frames).

All the fMRI data were preprocessed by AFNI, FSL, and SPM. The data with excessive motion resulting in translation greater than 3 mm, rotation greater than 3°, and a mean frame displacement (FD) exceeding 0.5 mm were excluded. In the preprocessing stage, all of the fMRI datasets were subjected to motion correction with the Friston 24-parameter model (Friston, Williams, Howard, Frackowiak, & Turner, 1996), skull-stripping, slice-timing, despiking, and detrending. For the anatomical information, native fMRI images were registered to the native T_1 -weighted image and segmented into white matter (WM), gray matter (GM), and cerebrospinal fluid (CSF). The fMRI datasets were spatially normalized to a standard Montreal Neurological Institute (MNI) template and resampled to an isotropic resolution of $2 \times 2 \times 2$ mm³. Then, a linear detrend was applied to eliminate any signal drift induced by system instability. Finally, the effects of nuisance regressors, including the six motion parameters, respiration/cardiac pulsations, WM, and CSF, were removed from the preprocessed datasets. The PMU data points within each TR were averaged for the physiological denoising. Since not all participants had intact PMU recordings during both the awake and sleep sessions, we regressed out the nuisance regressors whenever applicable (Table S2). The preprocessed data were temporally bandpass filtered between 0.01 Hz and 0.1 Hz, and then smoothed with a Gaussian kernel (FWHM = 6 mm) to improve the signal-to-noise ratio.

2.4 | Dynamic functional connectivity analysis

The ROI-based dFC was generated by using the DynamicBC toolbox and applied separately to the fMRI sessions of each stage (Liao et al.,

2014). The sliding-window approach (window size = 50 TRs, step size = 10 TRs) was performed to disassemble the BOLD time course. If the remaining frames for the sliding-window were less than the window size, then the data would be discarded for the analysis. Next, the region-to-region connectivity in each window was calculated, resulting in multiple time-varying connectivity strengths in each session (i.e., dFC). Cortical regions were extracted from a 17-network cortical parcellation estimated in 1000 young adults (Yeo et al., 2011) and the subcortical regions were from ASEG (Fischl, Salat, Busa, Albert, & Dieterich, 2002) with a total of 128 ROI nodes, resulting in 8128 edges in total. The mean BOLD time series of each ROI was extracted from the preprocessed fMRI data. The mean BOLD time series of all voxels within each ROI was averaged, and then the Pearson's correlation coefficients were calculated in a pairwise manner between the mean time series of all ROI pairs. These correlation coefficients, considered the dFC strength, were transformed into Z-scores using Fisher's Z formula for statistical analysis.

2.5 | Statistical comparison of dFC among sleep stages

The mean and variance of dFC within every sliding-window for each nonoverlapped sleep stage were calculated individually for each participant. Subsequently, the mean-variance relationship for dFC in each sleep stage was evaluated with all the connections averaged over all of the participants. A high strength for the dFC indicated rich network interaction (Friston et al., 2004), whereas a high variance in the dFC indicated network connection instability and the underlying rich information transfer between regions (Peraki & Servetto, 2004). The dFC_{var} was further divided into the $dFC_{var-within}$ and $dFC_{var-between}$, according to the intra-network and inter-network nodes, respectively.

The changes of the Z-transformed dFC distributions were described using skewness and kurtosis to estimate their statistical properties across stages. Skewness is a measure of the asymmetry of a probability distribution. The formula for skewness is as follows:

$$\text{skewness} = \frac{\sum_{i=1}^N (Y_i - \bar{Y})^3 / N}{s^3}, \text{ where } \bar{Y} \text{ is the mean, } s \text{ is the standard deviation, and } N \text{ is the number of data points.}$$

Skewness for a normal distribution is zero, and that for symmetric data is almost zero. Positive values for skewness indicate data that are skewed right, and vice versa, where "skewed right" means that the left tail is longer than the right tail. Elevated skewness for an FC distribution indicates decreased strong connections (Buzsáki & Mizuseki, 2014). Meanwhile, kurtosis is a measure of whether data are heavy-tailed or light-tailed relative to a normal distribution. Data sets with low kurtosis tend to have light tails or lack outliers. The formula for kurtosis is as follows:

$$\text{kurtosis} = \frac{\sum_{i=1}^N (Y_i - \bar{Y})^4 / N}{s^4}, \text{ where } \bar{Y} \text{ is the mean, } s \text{ is the standard deviation, and } N \text{ is the number of data points.}$$

We used the paired t-test to evaluate the difference in every Fisher's Z-transformed dFC between sleep stages. The results were

displayed with family-wise error (FWE) correction using Network Based Statistics (NBS) (Zalesky, Fornito, & Bullmore, 2010). To highlight the changes in sleep compared to the N0 stage, we further calculated the differences in Fisher's Z-transformed dFC between the N0 stage and each sleep stage. We averaged the mean/variance of the dFC that belonged to the same subnetwork as the within network mean/variance. In the same way, we averaged the mean/variance of the dFC for different subnetwork as the between network mean/variance. The 18 subnetworks were defined as the combination of 17-network parcellation (Yeo et al., 2011) and the subcortical regions (Figure 1).

3 | RESULTS

3.1 | Mean-variance relationship across sleep stages

The dFC_{mean} and dFC_{var} were calculated for all the connections (8,128 edges). Figure 2a shows the global relationships between dFC_{mean} and dFC_{var} across the four wake-sleep stages. The relationship between dFC_{mean} and dFC_{var} presented a negative correlation in general, but the quadratic fitting variables changed across the four stages. The dFC_{mean} gradually decreased along with the increasing depth of sleep and reached the lowest level at the N3 stage (Figure 2b), whereas dFC_{var} peaked at the N2 stage and reached its lowest level at the N1 stage (Figure 2c). The distribution properties across the sleep stages were quantified as the distribution parameters (skewness and kurtosis) of dFC_{mean} and dFC_{var} across the four sleep stages. Compared with the near-zero skewness at the N0 and N1 stages, the skewness of the dFC_{mean} distribution was significantly increased at the N2 and N3 stages (Figure 2d,e; $p < .05$ with Bonferroni correction). In contrast, the dFC_{var} distribution was significantly decreased in skewness and kurtosis in the N2 stage compared with in the N0 and N1 stages (Figure 2f,g; $p < .05$ with Bonferroni correction).

3.2 | Stage-dependent disparity in dFC

Figure 3 illustrates the stage changes in dFC_{mean} and dFC_{var} in contrast to the N0 stage. Significantly higher dFC_{var} and lower dFC_{mean} were prominent in deep sleep (i.e., the N2 and N3 stages) compared with wakefulness. Among 8,218 edges in total, 480 and 1,490 edges in the N2 stage showed significantly lower dFC_{mean} (Figure 3b, red dots) and higher dFC_{var} (Figure 3b, green dots), respectively, compared with the N0 stage. However, for the N3 stage, 2,898 and 254 edges presented significantly lower dFC_{mean} and higher dFC_{var} , respectively, compared with the N0 stage ($p < .05$ with the FWE correction). Moreover, compared with the N0 stage, 48 and 54 connections in the N2 and N3 stages, respectively, showed both significantly decreased dFC_{mean} and significantly increased dFC_{var} (Figure 3b yellow dots).

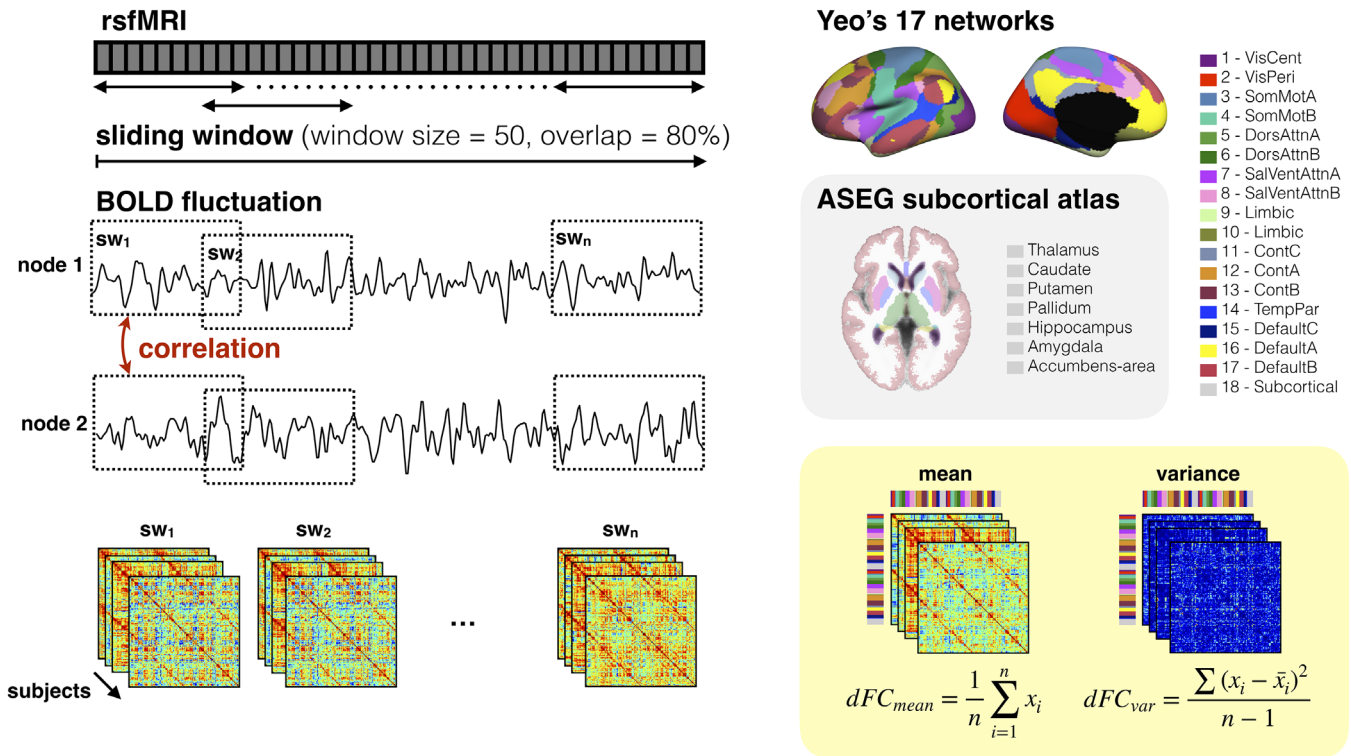


FIGURE 1 Workflow for dFC analysis. dFC was generated from each sleep stage using the sliding-window analysis (window size was 50 frames with 80% overlap), and the template comprised 128 ROIs, which consisted of Yeo's 17 function-based networks template and the ASEG subcortical atlas. The x_i and n denotes the FC within each window and the number of sliding window, respectively, whereas dFC_{mean} and dFC_{var} were calculated at each stage for all of the participants [Color figure can be viewed at wileyonlinelibrary.com]

3.3 | Network-based connectivity across sleep stages

Figure 4 demonstrates the dynamicity of the within- and between-network dFC_{mean} and dFC_{var} across the four sleep stages. Here we only presented the 17 cortical networks because combining all subcortical structures into single network might not be representative of multiverse subcortex functions. Instead, thalamocortical and hippocampal-cortical connectivity independently were shown in Figure S1. For the 17 cortical networks, all of the edges for dFC_{mean} and dFC_{var} were averaged within each network (Figure 4a,c for $dFC_{mean-within}$ and $dFC_{var-within}$, respectively). Similarly, between-network dFC_{mean} ($dFC_{mean-between}$, Figure 4b) and dFC_{var} ($dFC_{var-between}$, Figure 4d) were assessed through the node average across the networks. The $dFC_{mean-within}$ gradually decreased with the increasing depth of sleep in most of the networks (Figure 4a), including the somatosensory network, dorsal attention network, ventral attention network, and default mode network (DMN). In contrast, the $dFC_{mean-between}$ drastically decreased with deepening sleep (Figure 4b). However, the relationship between the N0 and N1 stages had different trends across networks, without significant differences. In terms of connectivity variations, the overall $dFC_{var-within}$ reached the maximum value at the N2 stage in most networks (Figure 4c), including the central and peripheral visual network, sensorimotor network, dorsal and ventral attention network, cognitive control network, and DMN. For all of the networks, the $dFC_{var-between}$ decreased from N0 to N1,

reached the maximum at N2, and then decreased at N3 (Figure 4d). Compared to the $dFC_{var-within}$, the $dFC_{var-between}$ presented a greater disparity between the N2 stage and the other stages.

4 | DISCUSSION

In this study, we observed that the multivariate relationship between the average magnitude of dFC (dFC_{mean}) and the variability of dFC (dFC_{var}) changed across sleep-wake states. Conceptually, in our study, dFC_{mean} represented the robustness of network integrity, and a gradually decreasing dFC_{mean} indicated the dissolution of network boundaries in sleep. Furthermore, dFC_{var} represented the instability of network connections, and increased dFC_{var} indicated swift switches in information propagation. Overall, we found that dFC_{mean} was slightly decreased with deepened sleep (N0~N1 > N2 > N3), whereas dFC_{var} changed across wake-sleep stages in a nonlinear manner (N0~N1 < N3 < N2). Decreased dFC_{mean} during sleep was accompanied by increased dFC_{var} . Elevated skewness for dFC_{mean} distributions in the N3 stage indicated that strong connections decreased along with an increased amount of low dFC_{mean} (Buzsáki & Mizuseki, 2014); moreover, this phenomenon also implied relatively low stationarity of FC during sleep (Thompson & Fransson, 2016). Our finding that the lowest dFC_{mean} occurred in the N3 stage was consistent with previous FC findings in NREM sleep (Spoomaker et al., 2010; Uehara et al., 2014), especially in terms of $dFC_{mean-between}$ (Larson-Prior et al., 2011;

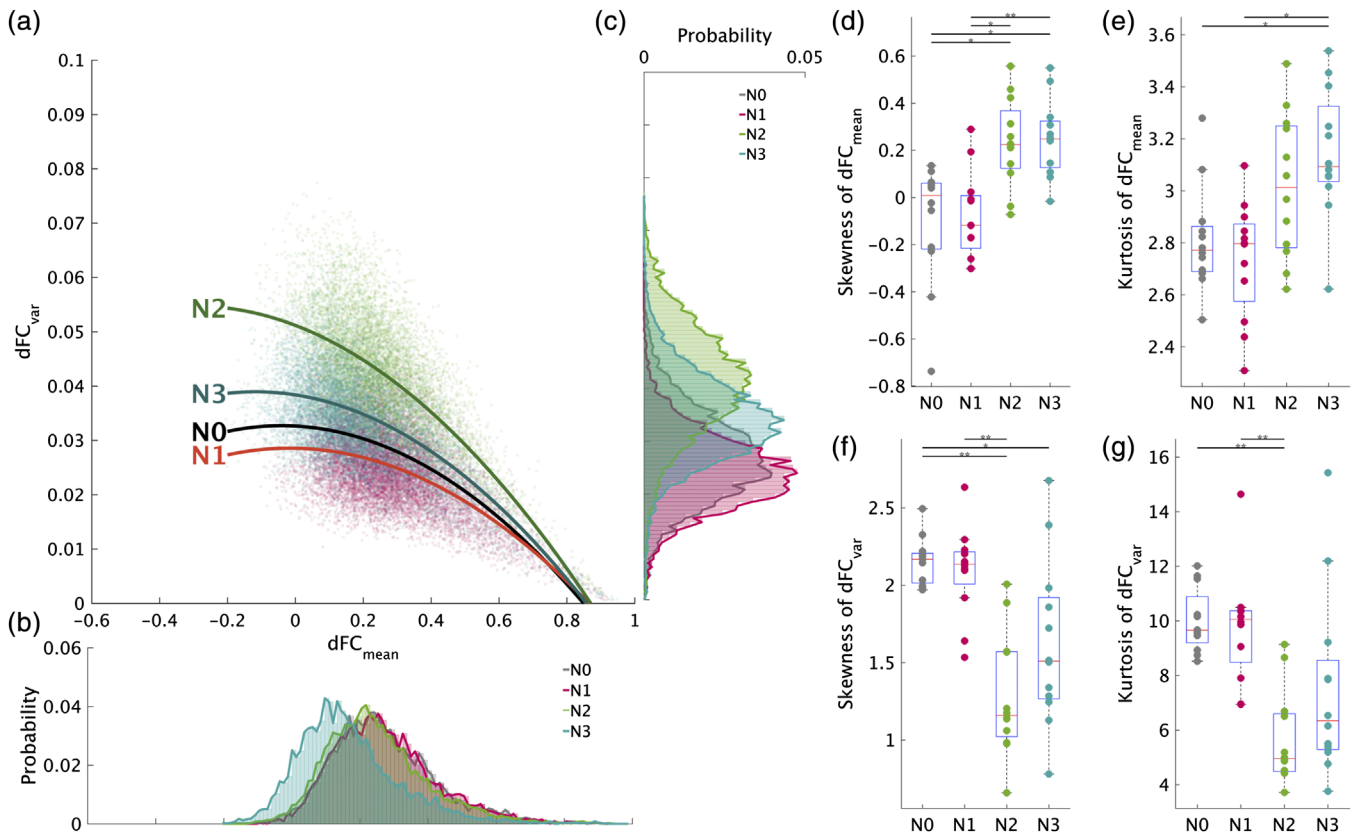


FIGURE 2 (a) The relationship between dFC_{mean} and dFC_{var} at each sleep stage. dFC_{mean} and dFC_{var} over the time series were calculated for all connections (8,128 edges) averaged across all of the participants. The data presented a negative correlation, we used quadratic fitting for mean–variance relationship ($r^2_{N0} = 0.31$, $r^2_{N1} = 0.32$, $r^2_{N2} = 0.47$, and $r^2_{N3} = 0.35$). The shift of the probability distribution across stages is shown in (b) dFC_{mean} and (c) dFC_{var} . (d) Skewness and (e) kurtosis for Z-transformed dFC_{mean} distributions across the four stages; (f) skewness and (g) kurtosis for Z-transformed dFC_{var} distributions across the four stages. (*sig. change and **sig. represent meaningful changes with NBS FWE corrected $p < .05$ and $p < .01$, respectively) [Color figure can be viewed at wileyonlinelibrary.com]

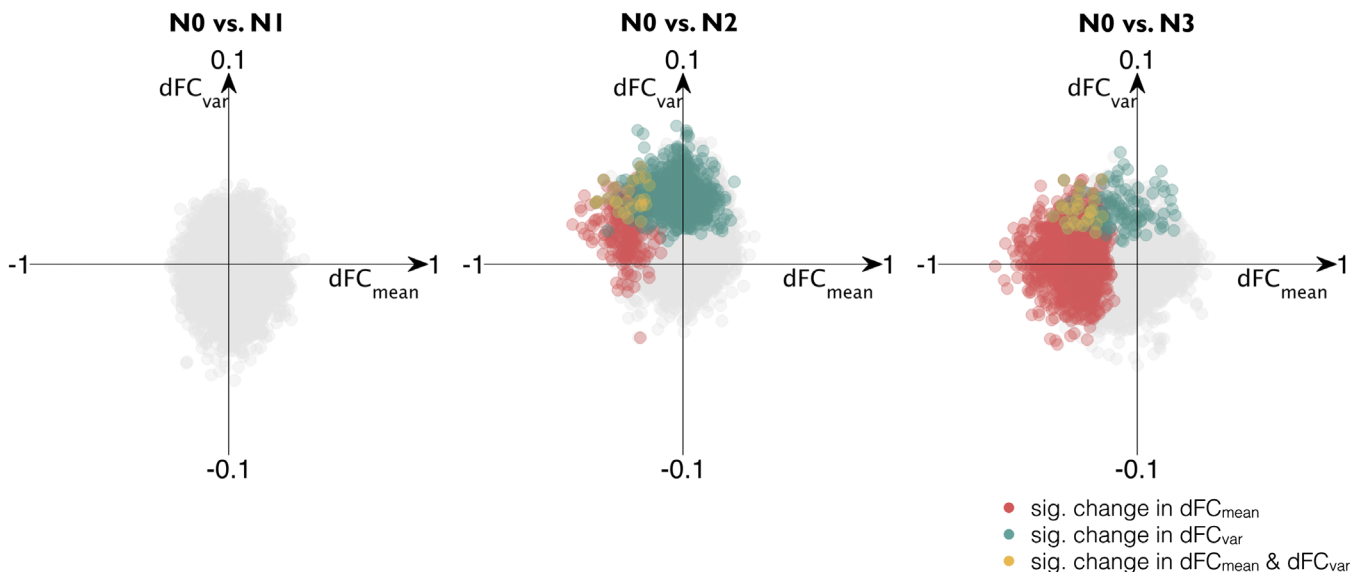


FIGURE 3 The dFC of NREM sleep stages (N1, N2, and N3) in comparison with wakefulness (N0). All of the connections of N0 are in the coordinates (0,0), and every dot presents the net differences at each sleep stages, compared with N0. The colored dots indicate significant connection differences from N0 (FWE corrected): red and green dots represent significant changes in dFC_{mean} and dFC_{var} , respectively, and yellow dots represent mean significant differences in N0, for both dFC_{mean} and dFC_{var} [Color figure can be viewed at wileyonlinelibrary.com]

Samann et al., 2011). As for dFC_{var} , we found that the highest instability occurred in the N2 stage (compared with N0 and N1 stages) and that this was associated with significant drops in both skewness and kurtosis, which was the most prominent phenomenon indicating the dynamic changes of brain integrity during NREM sleep.

4.1 | Resource reallocation for brain communication in sleep

A brain never rests, irrespective of whether it is in a waking or sleeping state, nor do neural communications ever cease. On the basis of this concept, researchers have proved that FC in sleep varies dynamically rather than remaining static (Haimovici et al., 2017; Spoormaker et al., 2010; Tagliazucchi, Crossley, Bullmore, & Laufs, 2016). Thus, dFC changes may indicate the subjective perceptions of consciousness, but this has rarely been studied in terms of dFC in sleep. Thompson et al. reported that, in the resting wakefulness condition, dFC_{mean} had a negative correlation with dFC_{var} according to sliding-window dynamic analysis (Thompson & Fransson, 2015), and similar observations in sleep were noted in our study. Thus, it is suggested that the dFC_{mean} - dFC_{var} relationship is constant across sleep-wake states. In other words, the trade-off between dFC_{mean} and dFC_{var} is evident in healthy human beings throughout the different stages of wakefulness and sleep: high dFC_{mean} has persistent long-distance connections with low instability (low dFC_{var}), and low dFC_{mean} corresponds to high dynamic variations in wakefulness. In the literature, dFC_{mean} in sleep has been reported to be decreased with increasing depths of sleep (Haimovici et al., 2017; Spoormaker

et al., 2010; Tagliazucchi et al., 2016), but dFC_{var} across the NREM sleep stages has not been revealed. In both states of staying awake (N0) and being asleep (N1), the low variance of dynamic connectivity implied a stationary integrity within functional networks, that is, temporal synchronization was robust within networks with high spatial specificity. For the N2 stage, the highest dFC_{var} and low dFC_{mean} demonstrate an alternative scenario in which specific within-network connectivity boundaries broke down and intrinsic information was distributed globally to inter-network brain regions, which agrees with the findings of increased unspecific connections in NREM sleep (Spoormaker et al., 2010). In contrast, during the N3 stage, the active long-distance communications were diminished and a relatively inactive condition persisted with residual local interactions. These macro-scale results might be linked to synaptic down-regulation in overall brain status during SWS (Tononi & Cirelli, 2006), a speculation supported by an earlier PET study that suggests a decrease in regional cerebral blood flow (rCBF) in most of the brain areas with deepening sleep (Braun et al., 1997; Maquet, 2000).

With respect to complexity, most studies have demonstrated that higher signal heterogeneity corresponds to richer information in the state of wakefulness compared to the low signal variability in SWS (Prete, Bolton, & Van De Ville, 2017). However, in this study, we focused on the variance of dFC, that is, the variability of temporal synchronizations, rather than the variability of signal itself. Our findings corresponded with those of previous studies (Tagliazucchi et al., 2014) in that we found that dFC_{var} was increased with the loss of consciousness. The disparity between signal complexity and dFC_{var} might reflect different definitions of the functional measurements, but

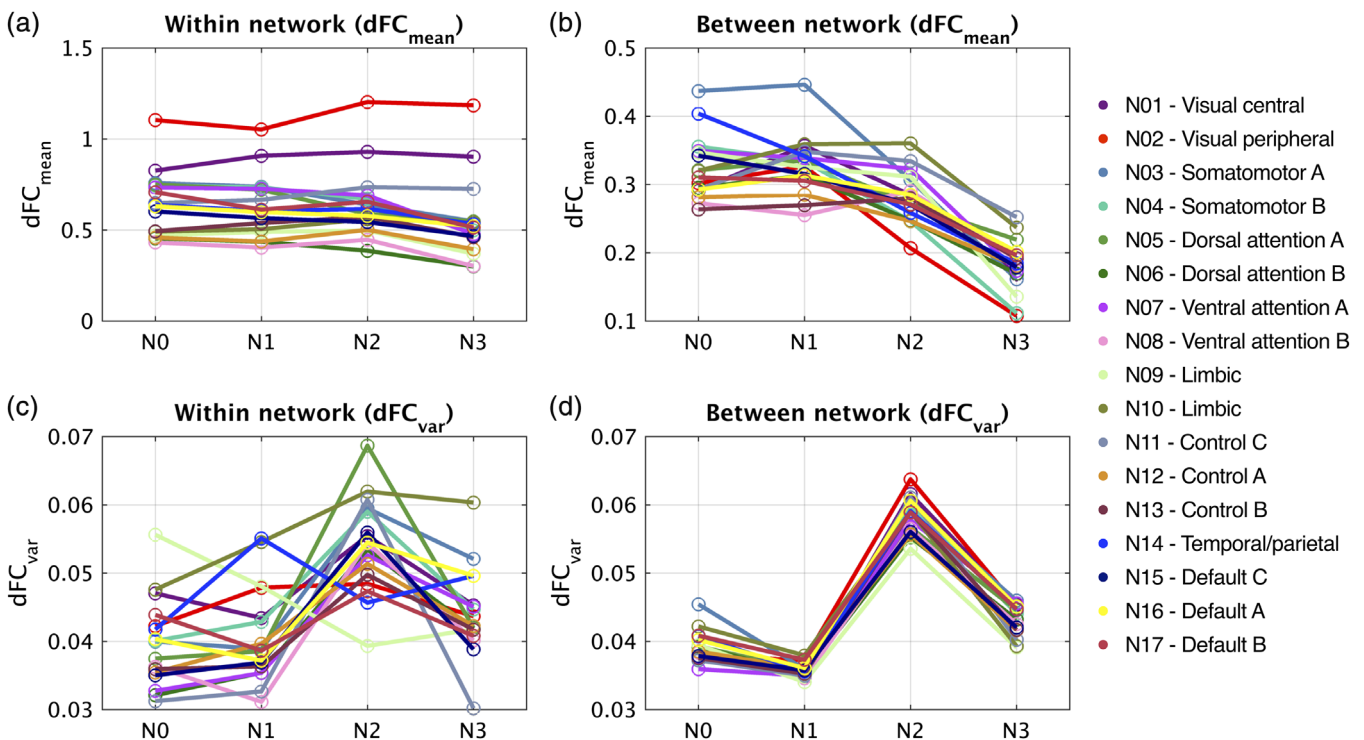


FIGURE 4 The cross-stage trend of 17 cortical networks in within- and between-network of (a, b) dFC_{mean} and (c, d) dFC_{var} . These networks were defined using Yeo's function-based cortical parcellation [Color figure can be viewed at wileyonlinelibrary.com]

this is beyond the scope of the current study. Future studies are required to clarify this point.

4.2 | Between- and within-network connectivity

We segregated the results into between- and within-network values (Figure 4) in order to assess dFC in terms of global or network-specific properties. The high consistency in $dFC_{\text{var-between}}$ across wake-sleep stages indicated the global disruption of network integrity at the N2 stage. With respect to within-network connectivity, the temporal-parietal and limbic networks presented distinct $dFC_{\text{var-within}}$ patterns. The temporal-parietal network presented the lowest variance at N0, higher variance at N1, and a gradual decrease in variance as sleep deepened. As for the limbic network in Yeo's 17-network cortical parcellation, the temporal pole (network 9) and orbitofrontal network (network 10) exhibited the lowest $dFC_{\text{var-within}}$ and highest $dFC_{\text{mean-within}}$ during the N2 stage, implying the highest information integration for emotional (Rempel-Clower, 2007) and sensorimotor associations at this stage (Rolls, 2004). The unimodal association area showed preserved rCBF during the N2 stage in previous PET studies (Braun et al., 1997; Maquet, 2000). Furthermore, the orbitofrontal cortex was related to sleep quality (Chao, Mohlenhoff, Weiner, & Neylan, 2014), sleep disorders (Joo, Tae, Kim, & Hong, 2009; Joo et al., 2010; Joo et al., 2011), and daytime sleepiness (Killgore, Schwab, Kipman, DelDonno, & Weber, 2012; Stoffers et al., 2012).

The physiological state of arousal is caused by the bottom-up regulation of cortical activation from the reticular activation system, which is derived from the brainstem, which, in turn, includes the thalamus and hypothalamus (Magoun, 1952). Our data presented the highest dFC_{mean} in the N1 stage and then gradually decreased with the increasing sleep depth in terms of thalamocortical connectivity (Figure S1). The altered thalamocortical FC during the N2 stage might be associated with K-complexes that inhibit arousal by suppressing the cortical activations of sensory inputs (Jahnke et al., 2012).

Awareness of the environment and the self was decreased with deepening NREM sleep (James, 1890; Laureys, 2005). Therefore, we evaluated the canonical functional networks associated with the awareness domain of consciousness. The DMN, comprising the PCC/precuneus, MPFC, and bilateral inferior parietal cortex (networks 15, 16, and 17), is related to self-awareness and conscious self-representation (Gusnard, Akbudak, Shulman, & Raichle, 2001). The DMN had the strongest FC at wakefulness, and the average $dFC_{\text{mean-within}}$ and $dFC_{\text{mean-between}}$ decreased with increasing depths of sleep. The PCC-MPFC connection decoupled and decreased during the N2 stage and troughed in the N3 stage, but the linkage between the bilateral parietal node in the DMN was strengthened at the N3 stage (Horovitz et al., 2008; Larson-Prior et al., 2009; Samann et al., 2011; Wu et al., 2012). Moreover, the dorsal attention network supports awareness of the environment and presented the same trend as the DMN. These results correspond with those of a previous study that observed that the DMN and attentional networks presented long-

range temporal correlations during wakefulness that were drastically diminished during the N3 stage (Tagliazucchi et al., 2013b). Other attention-related networks like the executive control network (ECN), ventral attention salience network, and cingulo-opercular network showed the same trend as the DMN as well. However, the ECN presented increased $dFC_{\text{mean-within}}$ in the N2 stage. During the N2 stage, the increased dFC_{mean} and dFC_{var} indicated increased but unstable temporal synchronizations in ECN, which was beyond our expectation and further analysis is warranted to provide explanations on the specific phenomenon.

Moreover, the peripheral and central visual network presented a distinct pattern in terms of dFC_{mean} , one that deviated from our main findings. As for the central visual network, both the $dFC_{\text{mean-between}}$ and $dFC_{\text{mean-within}}$ patterns were found to be increased in N1 sleep and then maintained at the same levels in the deep sleep stages, while the peripheral visual network drastically increased its $dFC_{\text{mean-within}}$ during N2 and N3 sleep. Such increased $dFC_{\text{mean-within}}$ in NREM sleep may play a role in NREM dreaming (Siclari, Larocque, Postle, & Tononi, 2013). Further studies are warranted to provide plausible explanations for the dynamic connectivity changes in the visual network.

4.3 | The IIT for consciousness in sleep

The capacity of information integration is critical for sleep functionality and consciousness according to the IIT. Our findings regarding dFC supported the notions of the IIT, similar to previous studies regarding SWS. First, a large-scale graph analysis indicates that the N2 stage presents a random network of organizations (Spoomaker et al., 2010) that limits its capacity to integrate information (Tononi, 2004). In contrast to the N2 stage, the large-scale functional brain network in SWS demonstrates both high local clustering and few long-range connections (Spoomaker et al., 2010; Uehara et al., 2014), which indicate the shrinkage of dFC_{var} toward a local connection that we observed in our results. Second, consciousness loss in SWS is associated with decreased integration ability corresponding to the IIT. Similarly, Deco et al. reported that stable but low signal integration occurred in SWS (Deco, Tagliazucchi, Laufs, Sanjuán, & Kringelbach, 2017). Third, Jobst et al. found that decreased effective connectivity indicates decreases in integration among brain regions in SWS (Jobst et al., 2017). These findings of dynamic analysis regarding the notion of information integration were compatible with the IIT of consciousness and were in agreement with our findings. In other words, high dFC_{mean} indicated stable brain network integrity as well as rich integration (Friston et al., 2004), whereas high dFC_{var} indicated the instability of functional synchronizations and information transfer. Furthermore, according to the information theory, higher instability corresponds with richer information (Peraki & Servetto, 2004). The underlying instability of information should be evaluated based on both $dFC_{\text{var-within}}$ and $dFC_{\text{var-between}}$ because dFC_{var} is more sensitive to the information transferred between networks (Thompson & Fransson, 2015). The fact that higher $dFC_{\text{var-within}}$ and the highest $dFC_{\text{var-between}}$ were observed in the N2 stage indicated the unstable transfer of information beyond

the predefined canonical networks along with a degraded information integration. Compared with the wakefulness (NO), dFC_{mean} decreased drastically but dFC_{var} increased slightly in SWS, indicating disrupted network organizations. We thus speculate that the stable within-network information integration is decreased in both the N2 and N3 sleep stages and replaced with unstable between-network information propagations.

Moreover, similar phenomena of dFC changes and consciousness loss have been noted in previous anesthesia studies. A decrease in prefrontal or subcortical connectivity was observed in PCC-centered coactivation patterns (Amico et al., 2014), with a decrease in dynamic complexity with consciousness loss. However, a contradictory finding following psilocybin intake revealed that the variability of FC between the left and right hippocampi was increased, with a larger space range being observed in each state over time (Tagliazucchi et al., 2014). Collectively, the consensus among various studies is that consciousness does not exist within specific brain networks, but emerges based on the persistence of FC (Horowitz et al., 2009; Samann et al., 2011; Spoomaker et al., 2010; Wu et al., 2012). As such, when the network specificity (dFC_{mean}) breaks down, the consciousness dissipates with increasing variability of information exchange (dFC_{var}).

4.4 | Limitations

In this study, we used the sliding-window approach to explore dFC in NREM sleep, which led to a study of brain dynamicity in human sleep. However, three confounding factors are worth noting for future investigations. First, for sleep evaluation, we employed the PSQI for sleep-quality assessments, but subjective ratings for conscious awareness were lacking. However, at the current stage, it is almost impossible to evaluate subjective consciousness levels at different sleep stages without interrupting participants' sleep. Second, the dFC analysis was based on the sliding-window cross-correlation method, without regarding effective causality in sleep. Former study has suggested that the causal relationship of cross-frequency signals between the cortex, thalamus, and hippocampus could be the key to refining long-term memory based on regional integrity (Staudigl et al., 2012). However, due to its invasiveness, this type of intracranial recording has never been conducted in normal human sleep. Future studies using refined and comprehensive experimental designs are thus warranted to elucidate memory consolidation in sleep. Third, the width of the sliding-window is critical for assessing dFC, and the window size of 125 s in 50 frames was chosen in the sliding-window analysis. Wilson et al. have investigated the epoch length in relation to FC in sleep (Wilson et al., 2015); however, sliding-window analysis has its limitations. It follows the criterion that the window size must have a greater amount of samples than the reciprocal of the underlying frequency component (Leonardi & Van De Ville, 2015). In other words, when using a short window size could lead to unstable and unreliable results, but using a long window size could result in any quick changes being missed. However, the $dFC_{\text{mean}}-dFC_{\text{var}}$ relationships across the wake-sleep states in this study did not change drastically with

different window sizes (62.5 s in 25 frames and 187.5 s in 75 frames). Related information has been included in Figure S2. At last, the simultaneously recorded PMU signal during the MR scans was not stable for every sleeping session. In this study, only one-third of the participants were with intact PMU recordings during both awake and sleep sessions that allowing remove respiration/cardiac pulsation noise for dFC analysis (Table S2). The number of connections, which significantly different from NO, changes with varying denoising approaches (Table S3). However, dFC persistently increased in variability (dFC_{var}) during N2 stage and mostly decreased in magnitude (dFC_{mean}) during N3 stage, showing that the main finding holds across different noise-removal methods. In summary, removal of physiological noise based on external recordings did not significantly impact the findings in the datasets.

5 | CONCLUSION

The current study provided a novel multivariate perspective to study the dynamic alterations of brain functions across wake-sleep stages. Rather than estimating decreases in the connectivity strengths of FC (dFC_{mean}), we evaluated the variations of FC (dFC_{var}) across the wake-sleep stages. The relative changes in dFC_{mean} and dFC_{var} reflect multivariate aspects of dynamic brain integrity in NREM sleep, implying distinct scenarios of consciousness dissipations. The results of the highest dFC_{var} and low dFC_{mean} in the N2 stage demonstrated that within-network boundaries were dissolved and intrinsic information was distributed globally with unstable synchronizations. Meanwhile, the observation of the lowest dFC_{mean} and low dFC_{var} in the N3 stage indicated a relatively inactive condition with residual local integration. These findings of dFC provide new insights for investigating brain integrity during NREM sleep.

ACKNOWLEDGMENTS

This research was funded by Taiwan Ministry of Science and Technology (MOST 104-2218-E-010-007-MY3, MOST 104-2420-H-038-001-MY3, MOST 105-2628-B-038-013-MY3, MOST 105-2632-H-038-001-MY3, MOST 106-2410-H-038-003-MY3, MOST 108-2420-H-010-001, MOST 108-2634-F-010-001), National Health Research Institutes (NHRI-EX108-10611E1), Shanghai Science and Technology Commission (17JC1404101, 17JC1404105), the Young Scientists Fund of the National Natural Science Foundation of China (81801774), and Natural Science Foundation of Shanghai (18ZR1403700), and further financially supported by the Brain Research Center, National Yang-Ming University from The Featured Areas Research Center Program within the framework of the Higher Education Sprout Project by the Ministry of Education (MOE) in Taiwan.

CONFLICT OF INTEREST

The authors declare no conflicts of interest.

ORCID

Yi-Chia Kung  <https://orcid.org/0000-0001-9295-7560>
 Timothy J. Lane  <https://orcid.org/0000-0002-8608-4270>
 Bharat Biswal  <https://orcid.org/0000-0002-3710-3500>
 Changwei W. Wu  <https://orcid.org/0000-0001-8968-9366>

REFERENCES

- Allen, E. A., Damaraju, E., Plis, S. M., Erhardt, E. B., Eichele, T., & Calhoun, V. D. (2012). Tracking whole-brain connectivity dynamics in the resting state. *Cerebral Cortex*, *24*, 663–676.
- Amico, E., Gómez, F., Di Perri, C., Vanhauzenhuyse, A., Lesenfants, D., Boveroux, P., ... Laureys, S. (2014). Posterior cingulate cortex-related co-activation patterns: A resting state fMRI study in Propofol-induced loss of consciousness. *PLoS One*, *9*, e100012–e100019.
- Beharelle, A. R., Kovačević, N., McIntosh, A. R., & Levine, B. (2012). Brain signal variability relates to stability of behavior after recovery from diffuse brain injury. *NeuroImage*, *60*, 1528–1537.
- Berry, R. B., Budhiraja, R., Gottlieb, D. J., Gozal, D., Iber, C., Kapur, V. K., ... American Academy of Sleep Medicine. (2012). Rules for scoring respiratory events in sleep: Update of the 2007 AASM manual for the scoring of sleep and associated events. Deliberations of the sleep apnea definitions task force of the American Academy of Sleep Medicine. *Journal of Clinical Sleep Medicine: JCSM: Official Publication of the American Academy of Sleep Medicine*, *8*, 597–619.
- Boly, M., Perlberg, V., Marrelec, G., Schabus, M., Laureys, S., Doyon, J., ... Benali, H. (2012). Hierarchical clustering of brain activity during human nonrapid eye movement sleep. *Proceedings of the National Academy of Sciences of the United States of America*, *109*, 5856–5861. <http://www.pnas.org/cgi/doi/10.1073/pnas.1111133109>
- Braun, A. R., Balkin, T. J., Wesenten, N. J., Carson, R. E., Varga, M., Baldwin, P., ... Herscovitch, P. (1997). Regional cerebral blood flow throughout the sleep-wake cycle. An H₂(15)O PET study. *Brain*, *120* (Pt 7), 1173–1197.
- Buzsáki, G. (1996). The hippocampo-neocortical dialogue. *Cerebral Cortex*, *6*, 81–92.
- Buzsáki, G., & Mizuseki, K. (2014). The log-dynamic brain: How skewed distributions affect network operations. *Nature Reviews. Neuroscience*, *15*, 264–278.
- Chang, C., Leopold, D. A., Schölvinck, M. L., Mandelkow, H., Picchioni, D., Liu, X., ... Duyn, J. H. (2016). Tracking brain arousal fluctuations with fMRI. *Proceedings of the National Academy of Sciences of the United States of America*, *113*, 4518–4523.
- Chang, C., Liu, Z., Chen, M. C., Liu, X., & Duyn, J. H. (2013). EEG correlates of time-varying BOLD functional connectivity. *NeuroImage*, *72*, 227–236.
- Chao, L. L., Mohlenhoff, B. S., Weiner, M. W., & Neylan, T. C. (2014). Associations between subjective sleep quality and brain volume in gulf war veterans. *37*, 445–452.
- Czisch, M., & Wehrle, R. (2009). Sleep. In *EEG-fMRI: Physiological basis, technique, and applications* (pp. 279–305). Berlin, Heidelberg: Springer.
- Deco, G., Tagliazucchi, E., Laufs, H., Sanjuán, A., & Kringelbach, M. L. (2017). Novel intrinsic ignition method measuring local-global integration characterizes wakefulness and deep sleep. *eNeuro*, *4*, ENEURO.0106–17.
- Feld, G. B., & Born, J. (2017). Sculpting memory during sleep: Concurrent consolidation and forgetting. *Current Opinion in Neurobiology*, *44*, 20–27.
- Fischl, B., Salat, D. H., Busa, E., Albert, M., & Dieterich, M. (2002). Whole brain segmentation: Automated labeling of neuroanatomical structures in the human brain. *Neuron*, *33*, 341–355.
- Friston, K. J. (2011). Functional and effective connectivity: A review. *Brain Connectivity*, *1*, 13–36.
- Friston, K. J., Frith, C. D., Dolan, R. J., Price, C. J., Zeki, S., Ashburner, J. T., & Penny, W. D. (2004). *Human brain function*. Cambridge, MA: Academic Press, Elsevier.
- Friston, K. J., Williams, S., Howard, R., Frackowiak, R. S., & Turner, R. (1996). Movement-related effects in fMRI time-series. *Magnetic Resonance in Medicine*, *35*, 346–355.
- Gusnard, D. A., Akbudak, E., Shulman, G. L., & Raichle, M. E. (2001). Medial prefrontal cortex and self-referential mental activity: Relation to a default mode of brain function. *98*, 4259–4264.
- Haimovici, A., Tagliazucchi, E., Balenzuela, P., & Laufs, H. (2017). On wakefulness fluctuations as a source of BOLD functional connectivity dynamics. *Scientific Reports*, *7*(1), 5908–5913.
- Hohwy, J. (2009). The neural correlates of consciousness: New experimental approaches needed? *Consciousness and Cognition*, *18*, 428–438.
- Horowitz, S. G., Braun, A. R., Carr, W. S., Picchioni, D., Balkin, T. J., Fukunaga, M., & Duyn, J. H. (2009). Decoupling of the brain's default mode network during deep sleep. *Proceedings of the National Academy of Sciences of the United States of America*, *106*, 11376–11381.
- Horowitz, S. G., Fukunaga, M., de Zwart, J. A., van Gelderen, P., Fulton, S. C., Balkin, T. J., & Duyn, J. H. (2008). Low frequency BOLD fluctuations during resting wakefulness and light sleep: A simultaneous EEG-fMRI study. *Human Brain Mapping*, *29*, 671–682.
- Iber, C., Ancoli-Israel, S., Chesson, A. L., & Quan, S. F. (2007). *The AASM manual for the scoring of sleep and associated events*. Westchester IL: American Academy of Sleep Medicine.
- Jahnke, K., Wegner von, F., Morzelewski, A., Borisov, S., Maischein, M., Steinmetz, H., & Laufs, H. (2012). To wake or not to wake? The two-sided nature of the human K-complex. *NeuroImage*, *59*, 1631–1638.
- James, W. (1890). *The principles of psychology*. New York: Cosimo.
- Jobst, B. M., Hindriks, R., Laufs, H., Tagliazucchi, E., Hahn, G., Ponce-Alvarez, A., ... Deco, G. (2017). Increased stability and breakdown of brain effective connectivity during slow-wave sleep: Mechanistic insights from whole-brain computational modelling. *Scientific Reports*, *7*, 4634.
- Joo, E. Y., Jeon, S., Lee, M., Kim, S. T., Yoon, U., Koo, D. L., ... Hong, S. B. (2011). Analysis of cortical thickness in narcolepsy patients with cataplexy. *34*, 1357–1364.
- Joo, E. Y., Tae, W. S., Kim, S. T., & Hong, S. B. (2009). Gray matter concentration abnormality in brains of narcolepsy patients. *Korean Journal of Radiology*, *10*, 552–558.
- Joo, E. Y., Tae, W. S., Lee, M. J., Kang, J. W., Park, H. S., Lee, J. Y., ... Hong, S. B. (2010). Reduced brain gray matter concentration in patients with obstructive sleep apnea syndrome. *33*, 235–241.
- Killgore, W. D. S., Schwab, Z. J., Kipman, M., DelDonno, S. R., & Weber, M. (2012). Voxel-based morphometric gray matter correlates of daytime sleepiness. *Neuroscience Letters*, *518*, 10–13.
- Larson-Prior, L. J., Power, J. D., Vincent, J. L., Nolan, T. S., Coalson, R. S., Zempel, J., ... Petersen, S. E. (2011). Modulation of the brain's functional network architecture in the transition from wake to sleep. In *Slow brain oscillations of sleep, resting state and vigilance* (pp. 277–294). Cambridge, MA: Elsevier. Progress in Brain Research Vol. 193.
- Larson-Prior, L. J., Zempel, J. M., Nolan, T. S., Prior, F. W., Snyder, A. Z., & Raichle, M. E. (2009). Cortical network functional connectivity in the descent to sleep. *Proceedings of the National Academy of Sciences of the United States of America*, *106*, 4489–4494.
- Laureys, S. (2005). The neural correlate of (un)awareness: Lessons from the vegetative state. *Trends in Cognitive Sciences*, *9*, 556–559.
- Lei, X., & Liao, K. (2017). Understanding the influences of EEG reference: A large-scale brain network perspective. *Frontiers in Neuroscience*, *11*, 205.
- Leonardi, N., & Van De Ville, D. (2015). On spurious and real fluctuations of dynamic functional connectivity during rest. *NeuroImage*, *104*, 430–436.

- Liao, W., Wu, G.-R., Xu, Q., Ji, G.-J., Zhang, Z., Zang, Y.-F., & Lu, G. (2014). DynamicBC: A MATLAB toolbox for dynamic brain connectome analysis, *4*, 780–790.
- Magoun, H. W. (1952). An ascending reticular activating system in the brain stem. *AMA Archives of Neurology and Psychiatry*, *67*, 145–154 discussion 167–71.
- Maquet, P. (2000). Functional neuroimaging of normal human sleep by positron emission tomography. *Journal of Sleep Research*, *9*, 207–231.
- Mulert C, Lemieux L (2009): . *EEG-fMRI: Physiological basis, technique, and applications*. Berlin, Heidelberg: Springer Berlin Heidelberg.
- Nir, Y., Massimini, M., Boly, M., Tononi, G. (2013). Sleep and consciousness. In *Neuroimaging of consciousness* (pp. 133–182). Berlin, Heidelberg: Springer Berlin Heidelberg.
- Nofzinger, E., Maquet, P., & Thorpy, M. J. (2013). *Neuroimaging of sleep and sleep disorders*. Cambridge, UK: Cambridge University Press.
- Peraki, C., Servetto, S. D. (2004). Capacity, stability and flows in large-scale random networks. ITW 2004.
- Preti, M. G., Bolton, T. A., & Van De Ville, D. (2017). The dynamic functional connectome: State-of-the-art and perspectives. *NeuroImage*, *160*, 41–54.
- Rasch, B., & Born, J. (2013). About sleep's role in memory. *Physiological Reviews*, *93*, 681–766.
- Rempel-Clower, N. L. (2007). Role of orbitofrontal cortex connections in emotion. *Annals of the New York Academy of Sciences*, *1121*, 72–86.
- Rolls, E. T. (2004). Convergence of sensory systems in the orbitofrontal cortex in primates and brain design for emotion. *The Anatomical Record. Part A, Discoveries in Molecular, Cellular, and Evolutionary Biology*, *281*, 1212–1225.
- Sämman, P. G., Wehrle, R., Hoehn, D., Spormaker, V. I., Peters, H., Tully, C., ... Czisch, M. (2011). Development of the brain's default mode network from wakefulness to slow wave sleep, *21*, 2082–2093.
- Siclari, F., Larocque, J. J., Postle, B. R., & Tononi, G. (2013). Assessing sleep consciousness within subjects using a serial awakening paradigm. *Frontiers in Psychology*, *4*, 542.
- Spormaker, V. I., Schröter, M. S., Gleiser, P. M., Andrade, K. C., Dresler, M., Wehrle, R., ... Czisch, M. (2010). Development of a large-scale functional brain network during human non-rapid eye movement sleep. *The Journal of Neuroscience*, *30*, 11379–11387.
- Staudigl, T., Zaehle, T., Voges, J., Hanslmayr, S., Esslinger, C., Hinrichs, H., ... Richardson-Klavehn, A. (2012). Memory signals from the thalamus early thalamocortical phase synchronization entrains gamma oscillations during long-term memory retrieval. *Neuropsychologia*, *50*, 3519–3527.
- Steriade, M. (2003). The corticothalamic system in sleep. *Frontiers in Bioscience*, *8*, d878–d899.
- Stoffers, D., Moens, S., Benjamins, J., van Tol, M.-J., Penninx, B. W. J. H., Veltman, D. J., ... van Someren, E. J. W. (2012). Orbitofrontal gray matter relates to early morning awakening: A neural correlate of insomnia complaints? *Frontiers in Neurology*, *3*, 105.
- Tagliazucchi, E., Carhart-Harris, R., Leech, R., Nutt, D., & Chialvo, D. R. (2014). Enhanced repertoire of brain dynamical states during the psychedelic experience. *Human Brain Mapping*, *35*, 5442–5456.
- Tagliazucchi, E., Crossley, N., Bullmore, E. T., & Laufs, H. (2016). Deep sleep divides the cortex into opposite modes of anatomical-functional coupling. *Brain Structure and Function*, *221*, 4221–4234.
- Tagliazucchi, E., & van Someren, E. J. W. (2017). The large-scale functional connectivity correlates of consciousness and arousal during the healthy and pathological human sleep cycle. *NeuroImage*, *160*, 1–18.
- Tagliazucchi, E., Wegner, v. F., Morzelewski, A., Brodbeck, V., Borisov, S., Jahnke, K., & Laufs, H. (2013a). Large-scale brain functional modularity is reflected in slow electroencephalographic rhythms across the human non-rapid eye movement sleep cycle. *NeuroImage*, *70*, 327–339.
- Tagliazucchi, E., Wegner, v. F., Morzelewski, A., Brodbeck, V., Jahnke, K., & Laufs, H. (2013b). Breakdown of long-range temporal dependence in default mode and attention networks during deep sleep. *Proceedings of the National Academy of Sciences of the United States of America*, *110*, 15419–15424.
- Thompson, G. J., Magnuson, M. E., Merritt, M. D., Schwarb, H., Pan, W.-J., McKinley, A., ... Keilholz, S. D. (2013). Short-time windows of correlation between large-scale functional brain networks predict vigilance intraindividually and interindividually. *Human Brain Mapping*, *34*, 3280–3298.
- Thompson, W. H., & Fransson, P. (2015). The mean–variance relationship reveals two possible strategies for dynamic brain connectivity analysis in fMRI. *Frontiers in Human Neuroscience*, *9*, 1–7.
- Thompson, W. H., & Fransson, P. (2016). On stabilizing the variance of dynamic functional brain connectivity time series. *Brain Connectivity*, *6*, 735–746.
- Tononi, G. (2004). An information integration theory of consciousness. *BMC Neuroscience*, *5*, 42.
- Tononi, G., Boly, M., Massimini, M., & Koch, C. (2016). Integrated information theory: From consciousness to its physical substrate. *Nature Reviews. Neuroscience*, *17*, 450–461.
- Tononi, G., & Cirelli, C. (2006). Sleep function and synaptic homeostasis. *Sleep Medicine Reviews*, *10*, 49–62.
- Tononi, G., & Koch, C. (2015). Consciousness: Here, there and everywhere? *Philosophical Transactions of the Royal Society of London. Series B, Biological Sciences*, *370*, 20140167–20140167.
- Uehara, T., Yamasaki, T., Okamoto, T., Koike, T., Kan, S., Miyauchi, S., ... Tobimatsu, S. (2014). Efficiency of a “small-world” brain network depends on consciousness level: A resting-state FMRI study, *24*, 1529–1539.
- Wang, C., Ong, J. L., Patanaik, A., Zhou, J., & Chee, M. W. L. (2016). Spontaneous eyelid closures link vigilance fluctuation with fMRI dynamic connectivity states, *113*, 9653–9658.
- Wilson, R. S., Mayhew, S. D., Rollings, D. T., Goldstone, A., Przewdzik, I., Arvanitis, T. N., & Bagshaw, A. P. (2015). Influence of epoch length on measurement of dynamic functional connectivity in wakefulness and behavioural validation in sleep. *NeuroImage*, *112*, 169–179.
- Wu, C. W., Liu, P.-Y., Tsai, P.-J., Wu, Y.-C., Hung, C.-S., Tsai, Y.-C., ... Lin, C.-P. (2012). Variations in connectivity in the sensorimotor and default-mode networks during the first nocturnal sleep cycle. *Brain Connectivity*, *2*, 177–190.
- Yeo, B. T. T., Krienen, F. M., Sepulcre, J., Sabuncu, M. R., Lashkari, D., Hollinshead, M., ... Buckner, R. L. (2011). The organization of the human cerebral cortex estimated by intrinsic functional connectivity. *Journal of Neurophysiology*, *106*, 1125–1165.
- Zalesky, A., Fornito, A., & Bullmore, E. T. (2010). Network-based statistic: Identifying differences in brain networks. *NeuroImage*, *53*, 1197–1207.

SUPPORTING INFORMATION

Additional supporting information may be found online in the Supporting Information section at the end of this article.

How to cite this article: Kung Y-C, Li C-W, Chen S, et al. Instability of brain connectivity during nonrapid eye movement sleep reflects altered properties of information integration. *Hum Brain Mapp*. 2019;40:3192–3202. <https://doi.org/10.1002/hbm.24590>